Efficient Cutting of Tapered Carbon Steels Using Wire Cut Process: Analysis and Multi-Objective Optimization

Pradipta Kumar Rout, Gangadhar Mande,
College of Engineering Bhubaneswar,Biju Patnaik University of Technology,Odisha,India

ABSTRACT

AISI 2010 carbon steel is a tool steel suitable for many uses. The industry is in dire need of figuring out the best process parameters for wire-cutting big metal slabs in order to maximize material removal rate while minimizing surface roughness and wire wear. The purpose of this study is to investigate how process variables affect tapered steel blank wire EDM. Wire EDM is used to manufacture tapered steel blanks with angles of 30°, 45°, and 60° and create holes in them. For this investigation, the controllable process parameters that are deemed to be within control are the pulse-off time, current, and taper angle; all other controllable parameters remain constant. Using the analysis of variance technique, the effects of these controllable parameters over the wire, MRR, kerf width, and surface polish are investigated. Additionally, regression models are created to relate the variables with the various controllable parameters for the four response variables. Multivariate optimization of The Genetic Algorithm is used to execute controlled parameters for favorable response variables.

Keywords: Kerf Width; Material Removal Rate; Surface Roughness; Wire EDM, Wire Wear

INTRODUCTION

Wire electro-discharge machining (EDM) is regarded as a modern variation of the non-traditional manufacturing process class. High intensity eroding sparks are used to machine metallic slabs and plates of increasing thickness utilizing a conductive wire (Sommer and Sommer, 2017). Within the machining set firstly, a metallic blank serves as an anode and a wire serves as a cathode. The metallic blank is dipped in a dielectric media and is cut through by the eroding sparks that come from the wire. As seen in Figure 1, the procedure involves feeding either consumable or non-consumable wire from a new spool to another wrapping spool while preserving enough tension between the two spools. The wire is controlled and fed normal to the blank's face (inw

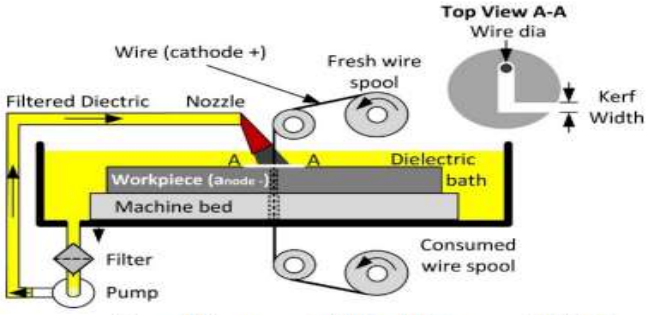

Figure 1 Components of Wire EDM process (WEDM)

Copper, brass, and tungsten are common wire materials used in wire EDM processes. On the other hand, aluminum, graphite, steel, copper, tungsten, inconel, and a variety of alloys based on titanium and bickel are common materials for work pieces (Sommer & Sommer, 2017; Asgar & Singholi, 2018). The most recent developments in research demonstrate wire experiments with low conductivity materials as well, including ceramics, metal, and polycrystalline diamond (PCD) (El-Hofy, 2005). The conventional dielectric in the system is ionized water, which makes it easier to protect the wire and blank interface and remove burrs from the erosion zone. High-frequency DC pulses initiate the blank erosion process by igniting a spark cycle that erodes the material into particles (Sommer and Sommer 2017).

CNC controlled wire EDM devices can create a wide range of intricate shapes and contours. Because of its great productivity in terms of exactitude and precision (Jameson, 2001).

Previous reviews of research comprise the most recent investigations on the WEDM method and are separated into two sections: the first discusses wire EDM on various materials, while the second section presents the wire EDM results on steels.

During the wire EDM of different materials, Gauri and Chakraborty (2009) used the Taguchi Method to investigate the impacts of pulse on time, wire feed, wire tension, peak current and delay time over the surface polish, as well as MRR and wire wear. Majumder and Saini (2017) optimized wire tension, wire feed, pulse rate, MRR, cutting speed, surface roughness, and kerf breadth using Ni-Ti alloy and titanium alloy (Ti-6Al-4V), respectively. Abhinesh et al. (2014) expanded the field of study by utilizing titanium alloy blanks and analyzing the MRR and wire wear outcomes by altering the wire's composition. By adjusting the wire cut's electrode ratio and speed capacitance for titanium alloys, Kumar and Singh (2018) extended their research investigation. Reddy et al. (2015) used the Grey method to diversify the examination of kerf width by substituting titanium with aluminum alloy HE30. Relationship Evaluation. The Taguchi Method was utilized by Rao et al. (2016) to increase the residual stress during the wire EDM of aluminum 2014 T6 alloy. During the wire EDM of aluminum 5754 alloy, Shihab (2018) improved the pulse rate and current for a better surface finish, a larger MRR, and the least amount of kerf width. For the metal matrix carbide, Shadab et al. (2019) optimized the wire winding rate, current, and pulse timing to achieve the maximum material removal rate and the best surface polish. Swiercz et al. (2019) performed the finite element analysis (FEA) and experiments to build wire EDM process model to observe the influence of wire-speed, flow rate of dielectric, and tension of wire over the kerf width formed. Numerous studies have used various approaches to cut the steel plates through the wire EDM process since there are a large

number of steel grades and a wide variety of applications. The features of this wide range of steel include varying melting points, thermal conductivity, and thermal expansion. It is ineffective to use the same WEDM process parameters for different steel alloys. As a result, numerous studies looked into the ideal parameters and provided mathematical models for various steel grades. The effects of wire travel, dielectric flow rate, wire tension, and pulse rate were examined by Huang and Liau (2003). rate during the wire EDM of SKD-11 steels over the surface finish and material removal rate. Liao et al. (2004) explored the impacts of spark frequency, surface roughness, and pulse rate throughout the width of the kerf while developing analytical models for the wire EDM over the Inconel (SKD11). His research was carried out by Kanlayasiri et al. (2007). For the increased surface roughness and adjusted pulse-peak current, pulse-on time, pulse-off time, and wire tension over cold die steel (DC53). Using feed rate and servo voltage as process parameters, Raksiri et al. (2010) analyzed and optimized the cutting thickness error for the Inconel (SKD-11) wire EDM. The wire EDM parameters were adjusted by Welling (2014) and Klacke et al. (2014) to increase the material removal rate and surface roughness for the Inconel 718. The frequency and vibration of the wire during the wire EDM of SKD-11 were observed by Kamei et al. (2016). Using a high-speed camera, they ascertained the impact of wire tension, deflection, and blank position on the vibration frequency and wire vibration. Takayama and colleagues (2016) enhanced the productivity of WEDM for cutting steel blanks (SKD-11) by using a closed-loop system, which raises the frequency of wire breaks and improves surface finish. For the Inconel 625, Babu and Soni (2017) employed a comparable experimental configuration. In order to increase the rate at which surface finish material is removed, Rajmohan and Kumar (2017) carried out a multi-variable optimization of pulse timing, current, wire feed rate, tension in the wire, and current. and kerf width created during Duplex Stainless Steel (DSS) wire EDM. Conde et al. (2018) examined the wire EDM result for D2 steel blanks by adjusting the blank height, dielectric pressure, and pulse off duration. Additionally, Sahoo et al. (2019) improved the primary parameter, kerf width, to increase the rate of material removal and surface finish when high-carbon and high-chromium steels are wire-EMBbed. The results suggested that the pulse width duration is the most important component, with the least influence coming from the wire input rate and pulse-off time. The Grey-Taguchi Technique was used by Priyadarshini et al. (2019a, 2019b) to obtain the optimal kerf width and MRR. through the optimization of the servo voltage and pulse timing in the wire EDM process of P20 steel (low carbon steel). They conducted additional study on the same material in a subcooled environment with comparable process settings and variables. Dayakar et al. (2019) optimized the wire EDM for low carbon steel using multiple variables, including pulse rate, peak current, and servo voltage. This resulted in improved surface roughness and material removal rate. (350). In order to link the process parameters with MRR and surface finish, they also created a regression model.Ahmed et al. (2020) used artificial neural networks (ANN) to optimize the pulse-on and pulse-off times for the highest and minimum surface roughness. In 2020, El-Bahloul carried out an analogous optimization for artificial intelligence (AI) technology in the AISI 304. Another optimization-based study was put forth by Arunadevi et al. (2021) to improve surface roughness and MRR.

This involved employing Decision Tree and Naive Bayes algorithms to optimize the process parameters.

The literature mentioned above reveals that the wire EDM procedure has been used to analyze a variety of metal alloys. The automotive and aerospace industries widely use steel AISI 1020, a low carbon general-purpose steel. Axles, camshafts, spindles, gears, and structural parts of machines Excellent machinability, weldability, and hardness (BHN between 119-235) make parts machineable. Due to its low carbon content, it has a low tensile strength range of 410–790 MPa (Dewangan et al., 2019). Because wire EDM has so many uses, it is inevitable to research its consequences. controllable factors that affect the crucial process results, include wire wear, kerf width, surface finish, and material removal rate (MRR). The effects of wire EDM across the various profile workpieces were not the subject of any of the research investigations that were previously described. These components are mostly used in complex cars and aircraft.components, machinery, and healthcare apparatus. In this study, tapered carbon steel alloy work parts have been taken into consideration due to industry requirements. The current investigation has examined the impact of the taper angle on the titanium alloy wire EDM results. It is clear from the literature analysis that using the same process parameter values for different steel grades does not always result in the best results. requires examining the results of wire EDM over a variety of cross-sectional blanks with complex shapes; for this reason, the same is taken into consideration in this study. In this study, four primary response variables—kerf width, surface roughness, wire wear, and MRR—were analyzed rather than just one or two outcomes. Distinct.To examine the impacts of taper angle, current, and pulse-off duration over these results, experimental setup and post-processing techniques were used. The study also presents the mean responses of the variables, an ANOVA, and a thorough commentary. After developing a regression model for each of the four response variables, the multi-variable/multi-objective process parameter optimization was used to get the desired results.

EXPERIMENTAL SET-UP

Finding the ideal wire EDM process settings for enhanced response outcomes of kerf width, surface roughness, MRR, and wire wear for tapered blanks of AISI 1020 steel sheets is the anticipated result of this research. A thorough research approach that includes an experimental design, results analysis,and further information is provided below.

Wire Cut Machine Tool

Utilizing a CHMER wire cut machine tool (type CW-43F), the envelope measured 500 x 350 x 200 mm in the x, y, and z directions, respectively. The wire electrode type, dielectric medium, serve feed (V), pulse on time (µs), pulse off time (µs), peak current (A), wire feed rate (mm/min), wire tension (N), and flushing pressure (psi or bar) are the controllable wire EDM process parameters of this machine tool.

Tapered Blanks

It has been thought of using a single source for the carbon steel 1020 blank. Table 1 is a list of the steel's material properties. Carbon steel 1020 tapered blanks with angles of 30, 45, and 60 degrees are machined. To ensure precision in analysis and prevent biases, a duplicate of every blank is made. Six blanks are therefore ready to be used to cut the slots in it. Figure 2 displays the samples' dimensions. The four slots that will be created on the blank by wire EDM are visible from the top perspective (Figure 2(a)). The front view (Figure 2(b)) of the blank shows that the t is per

Table 1. Material Properties of Carbon Steel 1020

Properties	Value
Chemical composition (%)	Mn(0.3), C(0.2), S(0.03), P(0.03). Fe(remaining)
Density (kg/m^3)	7870
Hardness (BHN)	111
Ultimate Tensile Strength (MPa)	380
Modulus of Elasticity (GPa)	200
Poisson's Ratio	0.29
Shear Modulus (GPa)	80
Specific Heat Capacity (J/g-°C)	0.486
Thermal Conductivity (W/m-K)	51.9
Melting Point (°C)	1500-1550

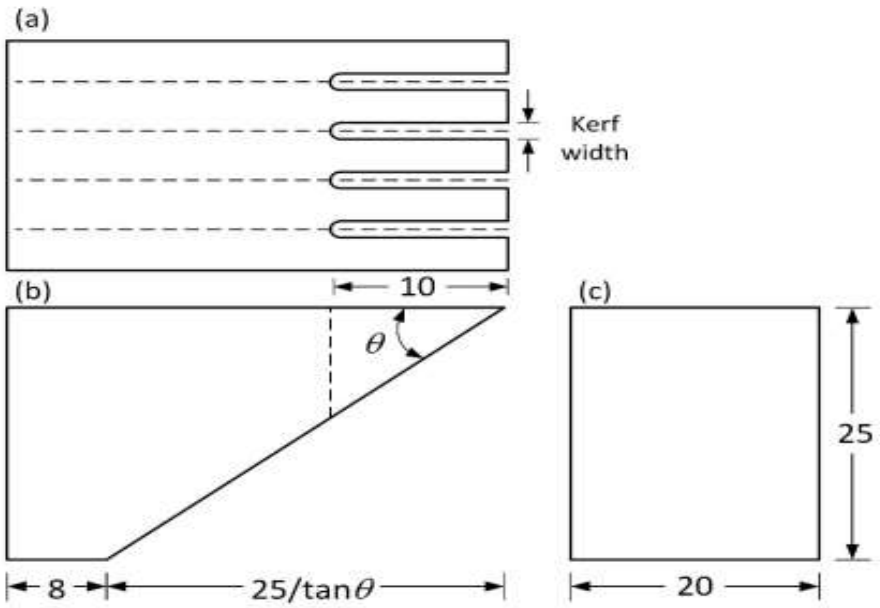

Figure 2 Tapped blank and slots cut through wire EDM, (a) top view, (b) Front view, (c) side view.

Experimental Design

In this study, several of the most important adjustable parameters—as listed in the literature review—are changed while maintaining constant values for the others. Table 2 lists these co8. controlled parameters and their corresponding levels.

Table 2. Controllable wire EDM process parameters

Parameters and Symbols	Levels		
	1	2	3
Taper Angle (A)	30°	45°	60°
Current (C)	5A	10A	--
Pulse-off time (POT)	20μs	40μs	--

f
times depend on one another. With a servo voltage of 65 volts and a pulse-on time of 25 s, a continuous feed rate of 3 mm/min is employed. With a wire velocity of 20 mm/min, the wire tension is set to 12N. Ionized water serves as the dielectric medium, and the flushing pressure rate is set at two liters per hour.

Twelve slots were to be generated, with a combination of parameters at all levels, and were to be replicated twice. A combination of configurable characteristics resulted in the generation of thirty-six slots in total. Thus, using the wire EDM, four holes were created on each of the nine carbon steel blanks. To reduce the bias in the results, these tests were conducted in a random order. Wire EDM was used to make four cuts on each blank, following the dashed lines as indicated in Figure 2(a), by adjusting the pulse off time and current setting.

Response Variable

The research's results, or response variables, are measured using the following method on the blank or wire used in the trials.

The width of the groove created by erosion is known as the kerf width (see Figure 1). Four different points along the slot's length are measured using the post-processing software after its magnified photos are captured with the digital microscope. Carbon steel 1020 tapered blanks are examined under the MM 500-T MTI corporate microscope, which has a DCM 310 digital camera connected. Figure 3 displays the images that were taken from the top view (see Figure 2(a).

The software Scope Photo 3.0 is used to process these photos and determine the kerf width along the slots. Kerf widths are measured at four different points along each slot's 10 mm length: 3 mm, 5 mm, 7 mm, and 10 mm from the flat face. The kerf widths are measured at each site,twice, indicating that the kerf widths are established as the ultimate kerf width. The wire EDM on the six blanks creates larger representations of the kerf width. In Figure 3, one of them is displayed.The efficiency of the wire EDM process can be determined using the material

removal rate (MRR), which is the ratio of the volume of metal removed to the machining time (Jameson 2001). Hence MRR can be determined by the following relation.

$$MRR = \frac{M_2 - M_1}{\rho \cdot t_{cut}} \quad (1)$$

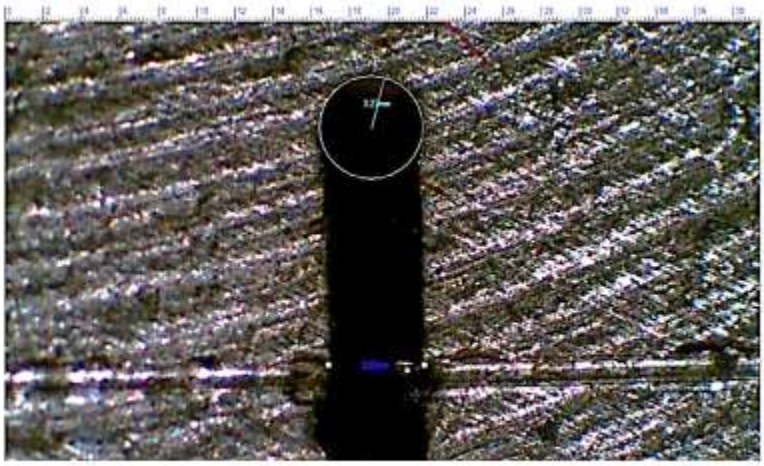

Figure 3 Kerf width of slot generated in blank with 45° taper angle (cut with Current 10A and POT 40µs)

Where, M2 and M1 are the masses of the blank before and after the cutting process, ρ is the density and tcut is the time spent on cutting the slot.

Since it influences the procedure's cost, the cost of the wire used is a crucial component of the wire EDM process. Depending on the kind of material being cut, more wire will be consumed at higher wire spooling and feed velocities. The percentage of wire used during the wire EDM process is measured by wire wear. To ensure accuracy when counting in limited spaces, high-precision digital balances with up to six digits are used to measure the masses of wire and blanks.

Surface integrity can be measured by evaluating the surface roughness exposed to erosion, which is an important step in the wire EDM process. An ideal waviness curve, according to James (2001), offers a better surface quality. After cutting the carbon steel blanks, as indicated in Figure 2(a), with a thin rotating saw from the center of the slots (dash lines), the roughness is measured without causing any damage to the eroded surfaces. Images of degraded surfaces are taken with the Meiji EMZ-8TR-PBH Zoom Stereo Microscope, which has a magnification range of 10 to 45X. Surface roughness is measured at three distinct heights of degraded surfaces using the Contouro Matic T2 high precision surface roughness gauge, which has a measurement capacity of up to 0.033µm. Both ongoing andmean readings are taken by moving stylus of the digital gauge at the heights of 30%, 60% and 90% of steel blanks, as shown in Figure 4.

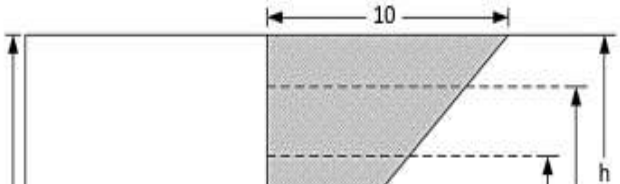

Table 3 presents the mean response variables determined with the combination of process parameters in order of running experiments.

Table 3. Mean response variables determined for the set of process parameters.

Taper Angle (Degree)	Current (Ampere)	Pulse off Time (µs)	Kerf Width (mm)	Surface Roughness (µs)	MRR (mm^3/min)	Wire Wear (Percentage)
30	5	20	0.4350	0.0133	11.85	0.1592
30	5	40	0.4388	0.0098	4.72	0.1936
30	10	20	0.4825	0.0150	13.45	0.1581
30	10	40	0.4950	0.0110	9.21	0.2169
45	5	20	0.2961	0.0163	6.27	0.3501
45	5	40	0.4088	0.0218	4.20	0.7867
45	10	20	0.3638	0.0193	11.97	0.3571
45	10	40	0.3536	0.0140	8.61	0.3978
60	5	20	0.2888	0.0120	5.03	0.5331
60	5	40	0.2913	0.0170	3.32	0.8866
60	10	20	0.3588	0.0175	8.40	0.3779
60	10	40	0.3613	0.0160	6.81	0.5523

The research's main hypothesis (Ho) states that the mean response variable found using various combinations of controllable parameters is equal, indicating that the response variable is not affected by any controllable parameters. According to the alternative hypothesis (H1), the means of the response variables vary depending on the interactions with other controllable parameters. With Table 2's established constraints for the controllable parameters, the hypotheses are tested over the 95% confidence interval.This shows that the response variable is significantly influenced by the factor or interaction. Each tapered blank of carbon steel 1020 is created with four slots using wire EDM, and the results are assessed using the response variables as detailed in the methodology section. Software for statistical analysis called Minitab is used to process the data pertaining to measured response variables and controllable parameters. Every one of the four answer variables is examined, and the findings are talked about below.

Kerf Width

Average kerf widths along the slots at various locations and generated through different combinations of parameters are shown in Figure 5. This figure shows that the largest kerf widths are generated in the blanks having the taper angles of 30°. Larger curve widths are formed due to the high rate of erosion on the exposed surfaces. This is caused due to the least surface area of the steel blank, exposed to the spark emitting wire. In comparison, small kerf widths are observed in the tapered blanks having angles of 45o and 60o , while not following the same trends. In both types of blanks, kerf width magnitude is majorly affected by the applied current. Higher kerf widths are observed in the blanks cut with 10A, whereas smaller kerf widths are seen cut with the 5A current. Although the kerf width remains stable during the wire EDM of steel blanks, in few cases an increase in kerf width can be seen at the higher distance from the flat face. This is due to the low visible surface area exposed to the spark emitting wire. Table 4 presents the analysis of variance (ANOVA) for the kerf width generated during the wire EDM of carbon steel 1020 by varying the process parameters. According to the P-value, less than 0.05 taper angle and current have substantial influence over the kerf width. Hence alternate hypothesis (H1) is valid for only these two process parameters. The taper angle has the largest effect of having F-value equal to 52.94, whereas current also affects the curve width having an F-value equal to 13.83. Other parameters and their interactions do not significantly impact the kerf width, which is evident from the P-values higher than the 5%.

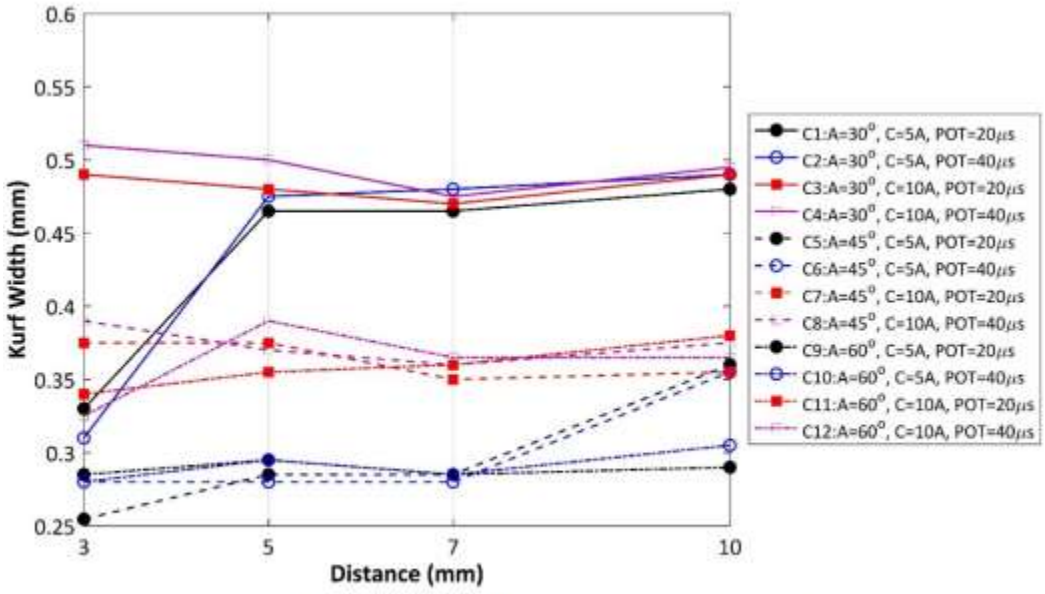

Figure 5 Mean kerf width along the length of the slot

Table 4. Analysis of Variance (ANOVA) for Kerf Width

Source	Degree of Freedom	Adjusted Sum of Squares	Mean Sum of Squares	F-Value	P-Value
Taper Angle (A)	2	0.083816	0.041908	52.94	0.000
Current (C)	1	0.010944	0.010944	13.83	0.003
Pulse-off Time (POT)	1	0.002552	0.002552	3.22	0.098
Taper Angle*Current	2	0.004316	0.002158	2.73	0.106
Taper Angle*Pulse-off Time	2	0.002845	0.001423	1.80	0.208
Current*Pulse-off Time	1	0.002168	0.002168	2.74	0.124
Taper Angle*Current*Pulse-off Time	2	0.005410	0.002705	3.42	0.067
Error	12	0.009499	0.000792		
Total	23				

Figure 6 illustrates how changing the process parameters affects the mean kerf width. Because of the increased surface area exposed to the eroding EDM wire, the figure illustrates how the mean kerf width reduces as the taper angle increases. The erosion density is spread due to the broad surface area exposed to the wire EDM. Leading to a reduction in the kerf width. Figure 6 illustrates how the high erosion rate caused by accumulated current causes the kerf width to expand, culminating in a huge kerf width. Figure 6 similarly shows that the kerf width increases as POT increases, however the F-value of the ANOVA is only 3.22, which is quite low when compared to the F-values for the taper angle and current. Thus, the outcome of POT is insignificant having a P-value < 0.05.

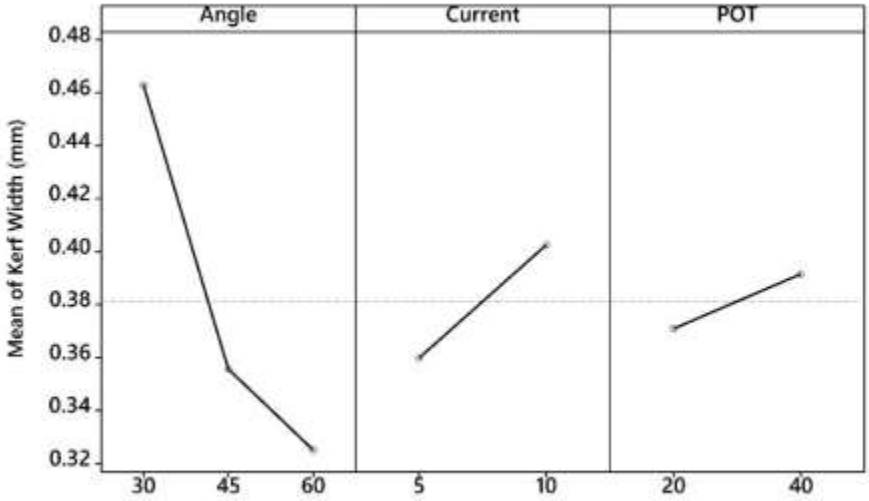

Figure 6 Main effects of mean kerf width

Surface Roughness

Analysis of Variance (ANOVA) for the surface roughness measured on the eroded carbon steel blanks is presented in Table 5. It suggests that none of the parameter and their interaction significantly has P-values higher than 5%. Due to the limited levels of parameters recommended for steel, the significance of process parameters and interactions seem minimal.

Table 5. Analysis of Variance (ANOVA) for surface roughness

Source	Degree of Freedom	Adjusted Sum of Squares	Mean Sum of Squares	F-Value	P-Value
Taper Angle (A)	2	0.0001262	0.0000631	3.06	0.084
Current (C)	1	0.0000012	0.0000012	0.06	0.812
Pulse-off Time (POT)	1	0.0000024	0.0000024	0.12	0.738
Taper Angle*Current	2	0.0000245	0.0000123	0.60	0.567
Taper Angle*Pulse-off Time	2	0.0000323	0.0000161	0.78	0.479
Current*Pulse-off Time	1	0.0000528	0.0000528	2.56	0.135
Taper angle*Current*Pulse-off Time	2	0.0000263	0.0000131	0.64	0.546
Error	12	0.0002472	0.0000206		
Total	23				

Material Removal Rate (MRR) Analysis of Variance (ANOVA) for MRR is presented in Table 6. A P-value less than 5% shows that the current, pulse-off time, taper angle, and taper angle/pulse-off time interact in order of their high F-values and influence and thus, have a significant impact over MRR. It depicts that the alternate hypothesis is valid for these parameters. Figure 8 shows the trend of MRR with varying WEDM parameters and indicates that with the increase in the taper angle, the material removal rate decreases. This is due to the fact that the surface area exposed to the eroding wire increases with the increase in taper angle. Hence, during the wire EDM process, emitting sparks are distributed over the increased surface area, causing a lower erosion rate. It results in decreased MRR over the large exposed surface area in higher taper angles. Figure 8 also illustrates that MRR enhances with the higher current and reduces with the higher pulse-off time. This is due to the high erosion rate at higher current and lower erosion rate due to the increase in pulse-off time.

The mean MRR fluctuation under the combined impact of controllable parameters is shown in Figure 9. Over MRR, the taper angle and pulse-off time interaction effect has the largest impact. Because of the low erosion rate and increases in the exposed area, MRR drastically decreases when the taper angle and pulse-off duration are increased. region of erosion. If the pulse-off time is set to 20µs, a larger declining rate is seen. P-values greater than 5% for other interaction effects indicate a negligible shift in the MRR (see Table 6).

Table 6. Analysis of Variance (ANOVA) for Material Removal Rate (MRR)

Source	Degree of Freedom	Adjusted Sum of Squares	Mean Sum of Squares	F-Value	P-Value
Taper Angle (A)	2	61.493	30.747	48.66	0.000
Current (C)	1	88.603	88.603	140.22	0.000
Pulse-off Time (POT)	1	67.445	67.445	106.73	0.000
Taper angle*Current	2	4.565	2.283	3.61	0.059
Taper Angle*Pulse-off Time	2	17.503	8.751	13.85	0.001
Current*Pulse-off Time	1	0.486	0.486	0.77	0.398
Taper angle*Current* Pulse-off Time	2	4.546	2.273	3.60	0.060
Error	12	7.583	0.632		
Total	23				

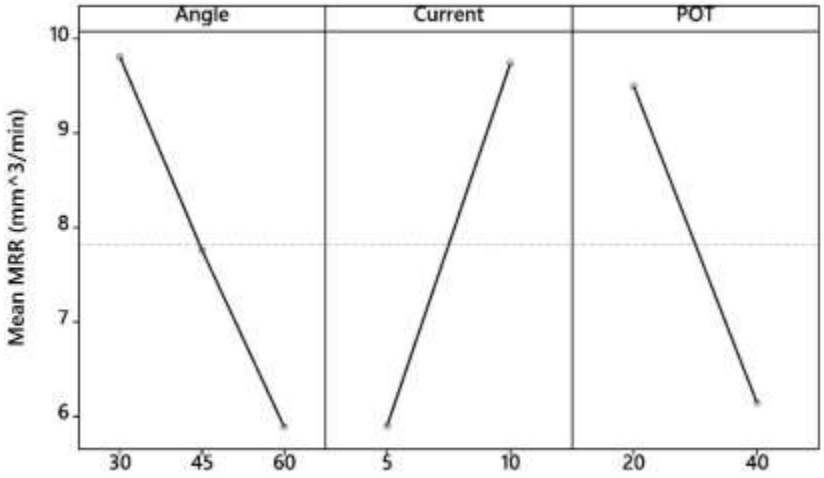

Figure 8 Main effects of mean MRR

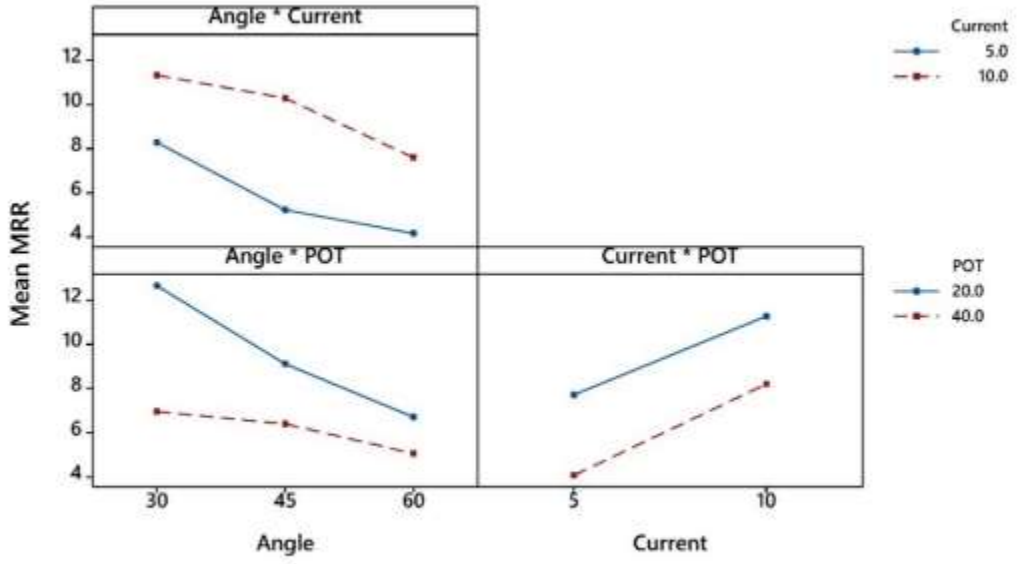

Figure 9 Interaction effects of mean MRR

Wire Wear Table 7 shows ANOVA for the wire wear during the wire EDM of carbon steel. It

Wire Wear

Table 7 shows ANOVA for the wire wear during the wire EDM of carbon steel. It shows that taper angle and current are significant over the wire wear, having P-values less than 0.05 and F-values 52.94 and 13.83 respectively.

Table 7. Analysis of Variance (ANOVA) for wire wear

Source	Degree of Freedom	Adjusted Sum of Squares	Mean Sum of Squares	F-Value	P-Value
Taper Angle (A)	2	0.083816	0.041908	52.94	0.000
Current (C)	1	0.010944	0.010944	13.83	0.003
Pulse-off Time (POT)	1	0.002552	0.002552	3.22	0.098
Taper Angle*Current	2	0.004316	0.002158	2.73	0.106
Taper Angle*Pulse-off Time	2	0.002845	0.001423	1.80	0.208
Current*Pulse-off Time	1	0.002168	0.002168	2.74	0.124
Taper Angle*Current*Pulse-off Time	2	0.005410	0.002705	3.42	0.067
Error	12	0.009499	0.000792		
Total	23				

Figure 10 presents the trend in wire wear with respect to controllable process parameters. It shows that increasing the taper angle increases the wire wear, which is due to the higher exposure of wire with the larger surface area during the wire EDM process. A high heat zone is formed around the wire during the WEDM process, whereby a small amount of current does not cause significant erosion. Instead, it disseminates in the form of heat. In the case of 10A current, the wire wear is decreased due to the effective erosion and its effective distribution over the exposed surface of the blank.

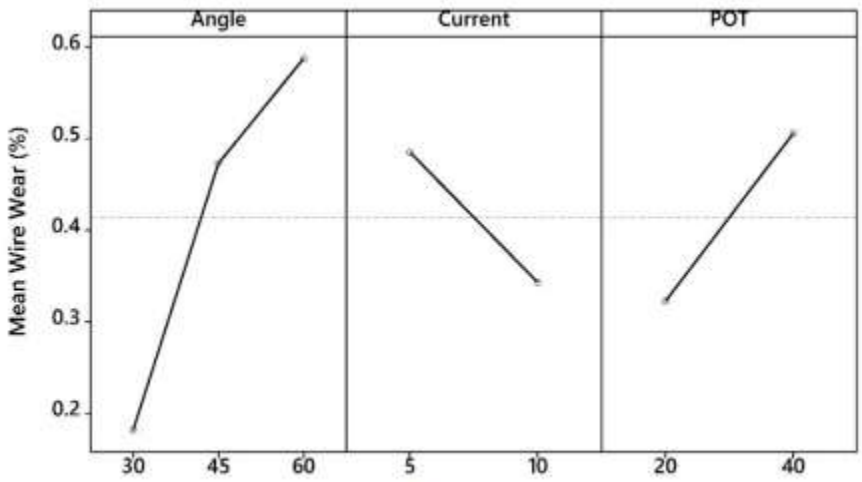

Figure 10 Main effects of mean wire wear

Multi-objective Optimization

Making use of NSGA-II The wire EDM's controllable parameters in this study are tailored to the favorable response characteristics. The MATLAB software's genetic algorithm function has been utilized to optimize each response variable separately in order to analyze the effects of the process parameters independently. The functions that correspond to the response variables for optimization are shown in the following equation.

$$f_1(p) = KW(A, C, POT) \quad (6)$$

$$f_2(p) = SR(A, C, POT) \quad (7)$$

$$f_3(p) = MRR(A, C, POT) \quad (8)$$

$$f_4(p) = WW(A, C, POT) \quad (9)$$

Where $\boldsymbol{p}$ denotes the process parameters collectively. The objective functions can be described as

$$z = \min [f_1(p) \quad f_2(p) \quad -f_3(p) \quad f_4(p)] \quad (11)$$

It should be noticed that since MRR is maximized in this case, the opposite function is minimized as indicated by − º. Level 1 and Level 2 of the current and pulse off time, as stated in 2, represent the maximum and lower bounds of optimization. For the 30°, 45°, and 60° taper angles, the outcomes of each individual optimization of each. Table 8 displays response variable.

Table 8. Optimized process parameters for minimization of individual response variable using GA.

Taper Angle (Degree)	Process Parameters		Kerf Width (mm)	Surface Roughness (µs)	MRR (mm^3/min)	Wire Wear (Percentage)
	Current (Ampere)	Pulse off Time (µs)				
30	5	40	0.3795(min)	0.0120	-5.185	0.3165
	10	40	0.3870	0.0092(min)	-9.180	0.2190
	10	20	0.4410	0.0156	-14.220(min)	0.2070
	5	20	0.3935	0.0125	-10.825	0.1245(min)
45	5	40	0.2445(min)	0.0189	-4.045	0.7395
	5	20	0.2885	0.0167(min)	-7.675	0.4275
	10	20	0.3435	0.0202	-11.265(min)	0.3825(min)
60	5	40	0.1995(min)	0.0182	-3.085	0.9825
	5	20	0.2735	0.0133(min)	-4.705	0.5505
	10	20	0.3360	0.0171	-8.490(min)	0.3780(min)

It can be seen from the table that the optimal process parameter providing the minimum value of one response variable does not guarantee the minimum response for the other variable. In a few cases, common minimal values are attained for the optimal parameters such as in the case of 45° taper angle cut with current 10A and pulse-off time of 20µs. A similar situation is observed in the 60° taper blank with parameter 10A 20µs. Hence, optimization of single response variable is not feasible, since it provides unacceptable results for the other response variables. A multi-variable, multi-objective Genetic Algorithm (GA) optimization has been applied using a computer prorgamme written in MATLAB software. NSGA-II algorithm is applied, which is a fast elitist sorting genetic algorithm to determine the optimal solutions for the minimization of objective function z. In the GA algorithm, parameters are set to the population size of 50, cross-over fraction 0.8, mutation fraction 0.4, elite count of population 0.05, and max iteration 200. The built-in function of Pareto optimal front offers multi-solutions, complying with the objective function z and hence provides a range of solutions. Since there are four different objective functions, which have entirely different trends as evident from Table 8, hence no single solution is possible for such problems, which is also confirmed in the literature (Mathworks, 2020; Simon, 2020). Using Pareto front, 19, 19, and 46, solutions were found based on the precision of up to 10-6 for each of the 30°, 45°, and 60° respectively. The results obtained through the hybridization with GA to obtain the local optimization is listed in Table 9. The response variable is not dominant and provides much better trade-off than the outcomes presented in Table 8. It also shows the percent change in the response variable as compared to these measured through the experimental results to the corresponding values. Such as, for the 30° taper angle work piece and the parameters 10A and 20µs, the measured four response variables from Table 4 are 0.4825mm, 0.015µm, 13.45mm3 /min and 0.1581%. Whereas, for the same blank, optimal parameters of 9.9894A and 20.25µs provide the variables 0.4402mm, 0.0154µm, 14.148 mm3/min, and 0.2069%. Hence, it corresponds changes of 9.61%, -3.18%, -4.94%, -23.62% in the response variable. The negative sign shows the decrease in response variable and the positive sign shows the increase. The decrease in response variables is the intended result in the case of kerf width, surface roughness, and wire wear due to minimization, whereas increases are favourable for the MRR due to intended maximization. It can be seen from the above table that the best results are achieved for the 30° taper angle work piece, where the kerf width is higher, whereas the least surface finish and wire wear are achieved with the best possible MRR. Table 9 shows the minimum kerf width, surface roughness, and wire wear and the maximum MRR. The most feasible values of current are near 10A for all the work pieces with any of the three taper angles. Whereas, pulse-off time around 20ms seems to be suitable for all three taper angle work pieces as evidenced by the optimization results.

Table 9. Multi-objectively optimized process parameters using the Genetic Algorithm.

Taper Angle (Degree)	Process Parameters		Kerf Width (mm)	Surface Roughness (µs)	MRR (mm^3/min)	Wire Wear (Percentage)
	Current (Ampere)	Pulse off Time (µs)				
30	9.9894	20.25	0.4402 (9.61%)	0.0154 (-3.18%)	14.148 (-4.94%)	0.2069 (-23.62%)
45	9.9987	20.01	0.3434 (5.92%)	0.0201 (-4.23%)	11.263 (6.82%)	0.3825 (-6.65%)
60	10.000	20.04615	0.3357 (6.87%)	0.0170 (2.48%)	8.4874 (-1.03%)	0.3786 (-0.18%)

Table 9 unequivocally demonstrates that the optimization findings propose a lower pulse-off time (20µs) and a larger current (10A) value. This runs counter to the optimization results that were shown for titanium, aluminum, and higher grades of steel, which indicate that occasionally larger pulse-off periods and lower currents are significant to allow the cutting interface to cool. If not, it leads to increased kerf breadth and surface roughness, which raises the metal's melting rate (Liao et al., 2004; Kumar and Singh, 2018; Wasif et al., 2020).

CONCLUSION

The effects of the wire EDM technique on the tapered blank of carbon steel 1020 have been investigated with respect to kerf width, surface roughness, MRR, and wire wear. The following conclusions can be made in light of the findings and the analysis that followed.

- In carbon steel 1020 taper blanks, the kerf width of the slots produced is significantly influenced by both taper angle and current. When the higher taper angle blanks are cut by the wire EDM, there is often a lesser rise in kerf width along the slot length.
- In carbon steel 1020, the relationship between the taper angle and the kerf width is inverse. The kerf width reduces as the taper angle increases. Additionally, it rises as the current increases while falling as the pulse-off time grows.
- Regarding the tapered blank's surface finish, no process parameter appears to have a significant influence.
- It can be because of the levels of the components chosen for this study, which are predicated on the suggested specifications for the steels.
- MRR is greatly impacted by the three adjustable process factors as well as the way the current and pulse-off time interact. Due to a greater region of exposure and more widespread erosion across a greater area, it diminishes as the taper angle and pulse-off duration increase concurrently.
- It becomes clear from the wire EDM of carbon steel 1020 that the taper angle and current have an impact on the wire wear. As the taper angle and current increase, the blank shows increased wire wear; nevertheless, the taper angle has a greater effect on wire wear than does the current.

- This study develops and presents the relationship between the response factors and the controlled wire EDM parameters, which can be used to forecast the wire EDM results.
- To obtain the optimal current and pulse-off time values for three distinct tapering blanks, the regression models are subjected to multi-objective optimization using a genetic algorithm. The best outcomes indicate that the lower pulse off time (20µs) and larger current (10A) offer favorable circumstances for all the
- four reaction variables as opposed to high-grade steel and titanium.

Regression models can be used to forecast wire wear, MRR, kerf width, and surface roughness under the ideal conditions. The data and analysis offered in this research can be implemented in the industry. Punches, other integral pieces, and the intricate die tool's geometries can be cut using these parameters utilized in machine tool components and other aviation parts. To achieve economy and productivity throughout the carbon steel 1020 production process, the ideal value of process parameters can be applied.

REFERENCES

Abinesh, P., Varatharajan, K., Kumar, G.S. 2014. Optimization of Process Parameters Influencing MRR, Surface Roughness and Electrode Wear During Machining of Titanium Alloys by WEDM, Int. J. Eng. Res. Gen. Sci. 2(4): 719-729.

Alduroobi, A.A.A., Ubaid, A.M., Tawfiq, M.A. et al. 2020. Wire EDM process optimization for machining AISI 1045 steel by use of Taguchi method, artificial neural network and analysis of variances. Int. J. Syst. Assur. Eng. Manag. 11: 1314–1338. DOI: https://doi.org/10.1007/s13198-020-00990-z

Asgar, M.E. and Singholi, A.K.S. 2018. Parameter study and optimization of WEDM process: A Review, IOP Conf. Series: Materials Science and Engineering 404, Lucknow, India.

Arunadevi Y. L, M., Prakash, C. P. S. 2021. Predicton of MRR & Surface Roughness in Wire EDM Machining using Decision Tree and Naive Bayes Algorithm, International Conference on Emerging Smart Computing and Informatics (ESCI), 2021, pp. 527-532, DOI: 10.1109/ESCI50559.2021.9396857.

Babu, T.V., Soni, J.S. 2017. Optimization of process parameters for surface roughness of Inconel625 in Wire EDM by using Taguchi and ANOVA method, Int. J. Curr. Eng. Technol. 7(3): 1127-1131.

Conde, A., Sanchez, J.A., Plaza, S., Ostolaza, M., Puerta, de la, Li, Z. 2018. Experimental Measurement of Wire-lag Effect and Its Relation with Signal Classification on Wire EDM, In Proceeding of the CIRP 68, Bilbao, Spain: 132-137. DOI: https://doi.org/10.1016/j.procir.2017.12.035

Dayakar, K., Krishnam Raju, K.V. M, Raju, C.R.B. 2019. Prediction and optimization of surface roughness and MRR in wire EDM of maraging steel 350, Materials Today 18(6): 2123-2131. DOI: https://doi.org/10.1016/j.matpr.2019.06.635

Dewangan, S., Mainwal, N., Khandelwal, M., Jadhav, P.S. 2019. Performance analysis of heat treated AISI 1020 steel samples on the basis of various destructive mechanical testing and microstructural behaviour, Aust. J. Mech. Eng. online: 2204-2253. DOI: 10.1080/14484846.2019.1664212.

El-Hofy, H. A. 2005. Advanced Machining Processes: Nontraditional and Hybrid Machining Processes, McGraw-Hill, USA.

El-Bahloul, S.A. 2020. Optimization of wire electrical discharge machining using statistical methods coupled with artificial intelligence techniques and soft computing. SN Appl. Sci. 2: 49. DOI: https://doi.org/10.1007/s42452-019-1849-6

Gauri, S.K. and Chakraborty, S. 2009. Optimisation of multiple responses for WEDM processes using weighted principal components, Int. J. Adv. Manu. Tech. 40: 1102–1110. DOI: 10.1007/s00170-008- 1429-1

Huang, J.T., Liao, Y.S. 2003. Optimization of machining parameters of Wire-EDM based on Grey relational and statistical analyses, Int. J. Prod. Res. 41(8): 1707-1720. https://doi.org/10.1080/1352816031000074973

Jameson, E. 2001. Electrical Discharge Machining, Society of Manufacturing Engineers (SME). USA. Muhammad Wasif, Syed Amir Iqbal, Yasir Ahmed Khan and Muhammad Tufail 190 Kamei, T., Okada, A., Okamoto, Y. 2016. High-speed Observation of Thin Wire Movement in Fine Wire EDM, In Proceeding of the 18th CIRP Conference on Electro Physical and Chemical Machining (ISEM XVIII), Tokyo, Japan, April 2016: 596-600. Kanlayasiri, K., Boonmung, S. 2007. Effects of wire-EDM machining variables on surf ace roughness of newly developed DC 53 die steel: Design of experiments and regression model, J. Mater. Process. Technol. 192: 459-464. Klocke, F., Welling, D., Klink, A., Veselovac, D., Nöthe, T., Perez, R. 2014. Evaluation of Advanced Wire-EDM Capabilities for the Manufacture of Fir Tree Slots in Inconel 718, In Proceeding of the 6th CIRP International Conference on High Performance Cutting (HPC 2014), Berkeley, USA, June 2014: 430-435. DOI: https://doi.org/10.1016/j.procir.2014.03.039 Kumar, R. and Singh, I. 2018. Productivity improvement of micro EDM process by improvised tool, Precis. Eng. 51: 529-535. Liao, Y.S., Yu, Y.P. 2014. Study of specific discharge energy in WEDM and its application, Int. J. Mach. Tools Manuf. 44(12): 1373-1380. https://doi.org/10.1016/j.ijmachtools.2004.04.008 Majumder, H. and Maity, K. 2017. Multi-Response Optimization of WEDM Process Parameters Using Taguchi Based Desirability Function Analysis, IOP Conf. Series: Material Science Engineering 338, Rourkela, India. Matheworks. 2020. Global Optimization Toolbox, MATLAB User's Guide, Mathworks Inc,

USA. Priyadarshini, M., Biswas, C.K., Behera, A. 2019. Machining of sub-cooled low carbon tool steel by wireEDM, Mater. Manuf. Process. 34(12): 1316-1325. DOI: https://doi.org/10.1080/10426914.2019.1662035 Priyadarshini, M., Biswas, C.K., Behera, A. 2019. Grey-Taguchi optimization of Wire-EDM parameters for P20 tool steel, In Proceeding of the 5th International Conference on Mechatronics and Robotics Engineering, ICMRE '19, Rome, Italy, February 2019: 5-8. DOI: https://doi.org/10.1145/3314493.3314506 Rao, P.S., Ramji, K., Satyanarayana, B. 2016. Effect of wire EDM conditions on generation of residual stresses in machining of aluminum 2014 T6 alloy, Alex. Eng. J. 55(2): 1077-1084. DOI: 10.1016/j.aej.2016.03.014 Rajmohan, K., Kumar, A.S. 2017. Experimental investigation and prediction of optimum process parameters of micro-wire-cut EDM of 2205 DSS, Int. J. Adv. Manuf. Tech. 93: 187-201. https://doi.org/ 10.1007/s00170-016-8615-3 Raksiri, C., Chatchaikulsiri, P. 2010. CNC Wire-Cut Parameter Optimized Determination of the Stair Shape Work piece, Int. J. Mech. Mechatron. Eng. 4(10): 924-929. Reddy, V.C., Deepthi, N., Jayakrishna, N. 2015. Multiple Response Optimization of Wire EDM on Aluminium HE30 by using Grey Relational Analysis' In Proceeding of the Materials Today 2(4–5), Hyderabad, India, February 2015: 2548-2554. DOI: https://doi.org/10.1016/j.matpr.2015.07.201 Sahoo, S.K., Naik, S.S., Rana, J. 2019. Experimental Analysis of Wire EDM Process Parameters for Micromachining of High Carbon High Chromium Steel by Using MOORA Technique, Micro and Nano Machining of Engineering Materials. Materials Forming, Machining and Tribology. Springer, Cham. DOI: 10.1007/978-3-319-99900-5_7 Shadab, M., Singh, R., Rai, R.N. 2019. Multi-objective Optimization of Wire Electrical Discharge Machining Process Parameters for Al5083/7% B4C Composite Using Metaheuristic Techniques, Arab. J. Sci. Eng. 44: 591. DOI: https://doi.org/10.1007/s13369-018-3491-9 Analysis and Multi-Objective Optimization of Wire Cut Process Parameters for Efficient Cutting of Tapered Carbon Steels Using Wire EDM 191 Shihab, S.K. 2018. Optimization of WEDM Process Parameters for Machining of Friction-StirWelded 5754 Aluminum Alloy Using Box–Behnken Design of RSM, Arab. J. Sci. Eng. 43: 5017-5027. DOI: https://doi.org/10.1007/s13369-018-3238-7 Simon, V. 2019. Multi-objective optimization of hypoid gears to improve operating characteristicsharacteristics', Mech. Mach. Theory. 146: 103727. DOI: 10.1016/j.mechmachtheory.2019.103727 Sommer, C. and Sommer, S. 2017. Complete EDM Handbook, 2nd ed., Advance Pub. Houstan, USA. Świercz, R., Oniszczuk-Świercz, D., Zawora, J., Marczak, M. 2019. Investigation of the Influence of Process Parameters on Shape Deviation after Wire Electrical Discharge Machining, Arch. Metall. Mater. 64(4): 1457-1462. DOI: 10.24425/amm.2019.130113 Takayama, Y., Makino, Y., Niu, Y., Uchida, H. 2016. The Latest Technology of Wire-cut EDM, In Proceeding of the CIRP 42: 623-626. DOI: 10.1016/j.procir.2016.02.259 Wasif, M., Iqbal, S.A., Fatima, A., Yaqoob, S., Tufail, M. 2020. Experimental investigation for the effects of wire EDM process parameters over the tapered cross-sectional work pieces of titanium alloys (Ti6Al-4V). Mech. Sci. 11: 221–232. DOI: https://doi.org/10.5194/ms-11-221-2020 Welling, D. 2014. Results of Surface Integrity and Fatigue Study of Wire-EDM Compared to Broaching and Grinding for Demanding Jet Engine Components Made of Inconel 718, In Proceeding of the 2nd CIRP Conference on Surface Integrity (CSI), Nottingham, UK, May 2014: 339-344. https://doi.org/10.1016/j.procir.2014.04.057